Cardiac pathology classification with one-dimensional convolutional neural network

Thomas Sponchiado Pastore[1], **Gabriel de Oliveira Ramos**[1], **Jean Schmith**[2,3,4]

[1]Graduate Program in Applied Computing, Universidade do Vale do Rio dos Sinos
São Leopoldo - RS, Brazil

[2]Polytechnic School, Universidade do Vale do Rio dos Sinos
São Leopoldo - RS, Brazil

[3]SENAI Innovation Institute for Sensor Systems (ISI-SIM)
São Leopoldo - RS, Brazil

[4]Competence Center on Digital Agriculture (EMBRAPII / SENAI-RS)
São Leopoldo - RS, Brazil

thomasSP@edu.unisinos.br, gdoramos@unisinos.br, JSCHMITH@unisinos.br

Abstract. *Currently, technology is indispensable in the medical field and the use of artificial intelligence tools is responsible for accelerating several processes, facilitating data acquisition, and recognizing important patterns for patient diagnosis. Focusing on cardiac pathologies, the electrocardiogram is the most widely used examination to diagnose patients, and optimizing this process is extremely important. Therefore, the objective of this study is to develop a model capable of classifying cardiac pathologies using raw ECG signals. For this purpose, signals from the PTB-XL database, recorded in the 12-lead standard, were used to train a 1D convolutional neural network without pre-training. Various hyperparameters were adjusted to find the model that is the best suited to the application. The model was evaluated using a test dataset, achieving an accuracy of 84%. The model demonstrated satisfactory performance, which can lead to the possibility of improving the current diagnostic system by accelerating the examination reading process and helping healthcare professionals interpret the results.*

1. Introduction

In recent years, there has been a growing search for efficiency, automation, and reduction of information loss in industries with the use of machine learning tools. The healthcare field also followed the same pattern, with studies looking for artificial intelligence solutions to diagnose pathologies and write medical documents. Machine learning algorithms (ML) are a great tool for recognizing patterns in complex data and creating predictions about new information. An example that is highly used and has a great capability of recognizing patterns, especially in image data, is the convolutional neural network (CNN) [Khan et al. 2020].

Although its usage is focused on image solutions, the CNN can be used in only one dimension when working with temporal series. The filter is modified to sweep along

the time axis and extract the features from the signal, this specific model is called 1D-CNN and also has a great capability of recognizing complex patterns, such as biomedical signals. These signals (ECG, EMG and EEG), are usually collected through electrodes that are placed on the patient's body and capture the potential difference between two regions, usually in millivolts. This signal can be measured in different regions of the body for a complete overview of the patient's condition.

Today, the eletrocardiogram (ECG) is one of the main exams used in hospitals for the diagnosis of cardiac pathology, the preoperative evaluation of the patient, and it also has a wide usage in the sports field in the evaluation of athletes. Given its importance, the exam must be quick and have an accurate interpretation. The ECG signal is usually formed by 5 waves (P, Q, R, S, T) that represent the cardiac cycle [Tortora and Derrickson 2018]. These waves are formed by potential differences generated by the sinoatrial node and spread throughout cardiac tissue, stimulating muscular activity. Pathologies associated with cardiac activity can usually be visualized through disturbances in the ECG signal in one or more leads, and their classification can be identified through different patterns using the wave's amplitude, duration, lack of waves, presence of lesion currents (J waves), or presence of duplicated waves.

The sinusal node sends a signal to the atrial muscle causing a contraction that excretes blood and fills the ventricle, represented in the ECG by the P wave. The signal travels through the atrioventricular node and his bundle until it reaches the interventricular septum [Wilmore et al. 2004] [Tortora and Derrickson 2018]. From the septum, the signal travels to the heart apex in 2 branches (left and right branches) that are considered the only electrical connection between the atrium and ventricle. The signal reaches Purkinje cells, being driven to the apex of the heart and from there to all ventricular cells rapidly (through gap junctions), signaling contraction of the ventricle, represented by the QRS complex[Tortora and Derrickson 2018]. Since there is a delay between the signal starting point and ventricle signaling, the atrium has the capacity to expel all blood to the relaxed ventricle before its contraction. With the start of ventricle contraction, the pressure inside the chamber increases until it exceeds the force of the semilunar valve, expels blood to the arteries with sufficient pressure to travel the body [Wilmore et al. 2004]. At the end of the contraction, the ventricle loses pressure to receive more blood from the atrium, filled with blood that accumulated while the ventricle was contracting, the relaxation of the ventricle is represented by the T wave in the ECG. From this point on, the cycle is repeated rhythmically to keep the blood oxygenated and flowing through the body [Wilmore et al. 2004] [Pastore et al. 2016].

Usually, when the ECG exam is performed, the electrodes are placed in specific points to provide the necessary information. The precordial derivations (represented by the letter "V") are recorded with electrodes located at 6 points in the chest, and 3 points, called indifferent, connected in the left leg and both arms (the Einthoven triangle points) [Pastore et al. 2016]. In the V1 and V2 records, the QRS complex is usually presented in the negative quadrant, since the electrodes are positioned at the base of the heart, where the signal starts and the currents flow away, traveling to the rest of the heart. The records V4, V5 and V6 has a QRS complex in the positive quadrant, since the currents usually flow to the apex. The V3 record is located above the heart apex, in this location the QRS complex is represented in both quadrants since the currents travel to the apex and from

there spread to the ventricle [Pastore et al. 2016]. Unipolar and bipolar derivations are also used to give important information about the patient, and in both derivations, the electrodes are positioned in the Einthoven triangle. The bipolar derivations are recorded between 2 electrodes measuring the potential difference between them, resulting in 3 records (I, II, III). Unipolar derivations are recorded between one positive electrode and the other two electrodes are considered negative, resulting in 3 records (aVF, aVR, aVL) [Tortora and Derrickson 2018].

Since these patterns are complex and hard to identify, machine learning tools can be used to recognize and classify pathologies, assisting healthcare professionals in the diagnosis process and accelerating crucial outcomes for patients. [Śmigiel et al. 2021] in their article use the PTB-XL database as used in the present paper and presented 3 methodologies to classify the signals: A convolutional neural network with entropy parameters, a convolutional neural network without entropy, and a SincNet model. The results show an accuracy of 89.2 % when classifying 2 classes, 76.5 % when classifying 5 classes, and 69.8 % when classifying 20 classes. [Bhanjaa and Khampariya 2023] used one-dimensional models based on AlexNet and LeNet models. Using the same database as the previous paper, the authors normalized the signals and filtered them using a Savitzky-Golay filter, achieving an accuracy of 97.5% with the AlexNet based model and 94.2% with the LeNet based model, showing a high capacity to classify ECG signals.[Bian et al. 2023] used an adapted one-dimensional Resnet-34 model with a handmade rule based neural network (HRNN). The authors used 2 databases with more than 20 thousand records with 8 waves each (I, II, V1, V2, V3, V4, V5, V6). The other 4 waves of the 12-lead standard exam were created computationally. The algorithm classifies the first database into 55 categories and the second in 34 categories, both achieving an F1-score and a recall near 90%. [Kusuma and Udayan 2020], in their article, observed various databases and methodologies to classify ECG signals. The 1D-CNN used by [Hasan and Bhattacharjee 2019] achieved a precision of 97.7 %, a sensitivity of 99.71 % and a specificity of 98.24 % in several datasets. They also used MLP models (multilayer perceptrons models) that achieve 88.7 % precision and CNN models that achieve results above 95% precision, concluding that CNN-1D was best suited for the application.

Therefore, the objective of this study is the development of a one-dimensional convolutional neural network algorithm to classify different cardiac pathologies using only the raw signal of a standard 12-lead ECG exam and the analysis of its performance compared to an experienced cardiologist diagnosis present in the database. In our experiments, we avoided complex signal filters to analyze the capacity of the 1D-CNN to classify ECG signals and make the process simple.

2. Materials and methods

To find the best solution for this classification problem, several artificial intelligence-based models were tested with different configurations until we found the best architecture results presented in this work. The results of these experiments were compared between them and with related papers to measure its classification potential across the 5 superclasses. Figure 1 shows a fluxogram of the methodology. The following sections describe each step of the methodology.

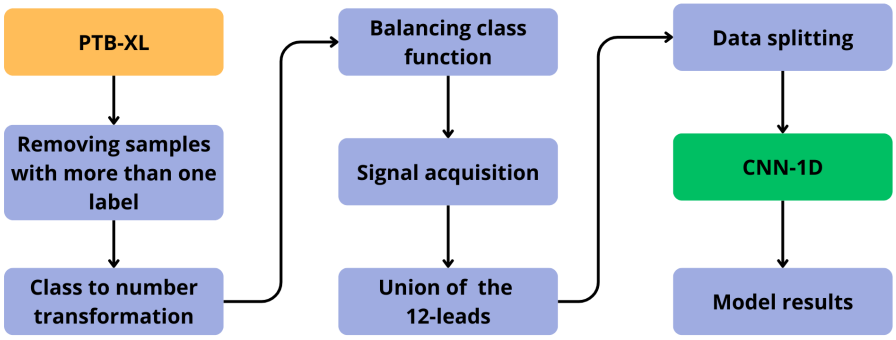

Figure 1. Fluxogram of the methodology.

2.1. Database

The PTB-XL database, found in the Physionet platform consists of 21837 records in a 12-lead standard format with a 10-second duration and a sampling rate of 100 Hz, being possible to extract 1000 points from each lead. The database also has other pieces of information, such as age, sex, height, weight, etc. [Wagner et al. 2020]. First, to use the records provided by the database, the signals with more than one classification were deleted, and the column of labels was transformed from string to numeric values. To read the records, the WFDB library (WaveForm DataBase) was used [Xie et al. 2022]. The result of each record is a matrix of 12 arrays with 1000 points each.

The dataset containing 16244 records (9069 "NORM", 535 "HYP", 1708 "CD", 2532 "MI" and 2400 "STTC" records) was randomly divided between the training set (80% of the samples) and the test set (20% of the samples), maintaining the proportion of classes in both sets. During training, the training set was split again, 20% of this set being destined to validate the model and adjust the weights of the model neurons in search of the best classification model [Fabian 2011].

The database presents 23 conditions that can be summarized in 5 great categories, also called superclasses [Wagner et al. 2020], namely HYP, CD, MI, STTC and NORM. These superclasses are our objective classification. Naturally, NORM refers to normal signals. Pathologies that fit the description of hypertrophy (HYP) alter the angles of the current vectors inside the heart, and in the ECG can be noticed by the change in amplitude and duration of waves in different records. Pathologies such as left and right ventricle hypertrophy, left and right atrial dilation, and interventricular septum hypertrophy are presented in this category [Kaplan et al. 1994] [Tsao et al. 2008].

The conduction disturbance (CD) superclass has a focus on blockages (complete and incomplete) in branches and fascicles. Pathologies such as the anterior and posterior right bundle of His branches blockage, the right and left bundle of His blockage, atrioventricular blockages, and Wolff-Parkinson-White syndrome [Nyholm et al. 2022] [Hall 2021]. Usually in light disturbances these pathologies have a longer duration in the QRS complex, and in more serious blockages there can be missing waves and deforma-

tions in the ST-T complex [Rose and Kuhn 2009]. when the blockage does not allow the passage of any signal from the atrium to the ventricle, Purkinje cells in the ventricle can start to generate their own signal, usually out of the rhythm of the atrium [Hall 2021].

The myocardial infarction (MI) superclass is divided into the location of the condition, separated into anterior, posterior, lateral, and inferior infarction. This condition occurs when cardiac tissue is damaged due to lack of blood flow through the coronary arteries. In early cases, it can present itself as complex Q and ST-T alterations, especially an increase in the T wave in at least 2 consecutive waves [Thygesen et al. 2012].

The last superclass is ST-T segment changes (STTC), which is characterized by anterior and posterior light ischemia, digitalic intoxication, also occurring in cases of Brugada syndrome or bad electrode position, sometimes being confused with myocardial infarction. In the records are presented by an inversion of T waves or biphasic waves [Hall 2021] [Thygesen et al. 2012].

2.2. Class balancing

Observing the data after the transformations, it is possible to notice a great disparity between the number of samples in each class. To avoid bias in model training and consequently ignore subtle changes related to pathologies, it was necessary to use a class balancing function.

This balancing can be done in 3 ways: oversampling (creating artificial signals for the minority classes), undersampling (deleting signals from the majority classes), or altering the weights of each class based on how much samples it has compared to all dataset [Maione et al. 2020] [Prati et al. 2003]. Both undersampling and oversampling have issues related to loss of data quality, since one of them would delete important pieces of information and the other would create new data that could be of inferior quality [Maccagnan et al. 2023], ruining the pattern that should be learned by the model [Prati et al. 2003].

Therefore, the class balancing function was implemented using the scykit-learn library. This function calculates the fraction of each class in the dataset and multiplies by the number of classes in the dataset, increasing the importance of minority classes in training and decreasing the importance of majoritarian classes to avoid biases in training stages [Fabian 2011] [Prati et al. 2003]

2.3. CNN model

Data were inputted into a one-dimensional convolutional neural network (1D-CNN), a model that can extract patterns from time series with low or no prepossessing. The model scans the series with a filter and performs the convolution between the signal and the filter values to create parameter maps that evidence patterns that are later classified using perceptron layers [Eren et al. 2019] [Lu et al. 2021]. [Wang et al. 2017] and [Fawaz 2020] based algorithm was used, where the input has 12000 points (format (1000, 12)) and the filters are randomly generated to create parameter maps that search for patterns in the signal [Ayadi et al. 2021] [Lu et al. 2021].

After each construction layer, the parameter map passes by 2 layers. The batch normalization, responsible for normalizing the values based on the mean and standard

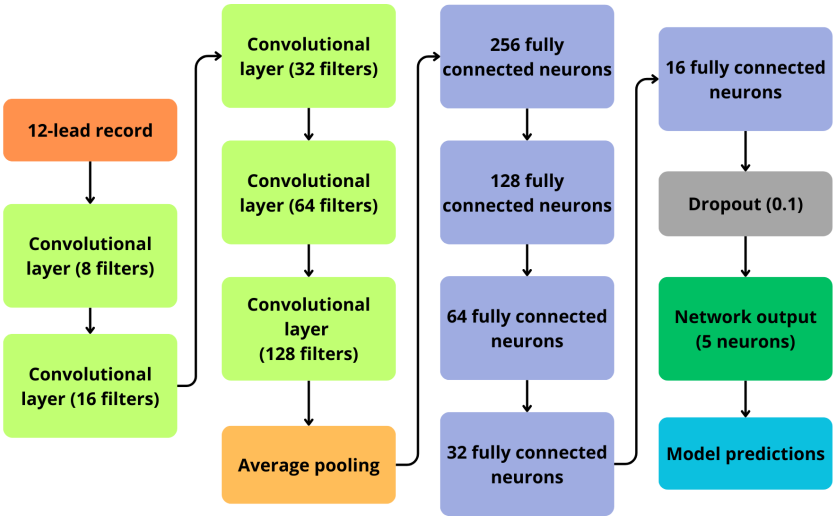

Figure 2. MLP model used at the top of the 1D-CNN.

deviation of a predetermined number of samples and the activation layer, that uses a function to alter the values that were input, creating a non-linear function, enabling the model to learn more complex patterns.

The network was formed by 5 convolutional layers, with increasing filters, kernel size of 3, the batch normalization value used was 32 samples, and the activation function was the RelU function, which maintains the value of the output if it is a positive value or alters the value to 0 if it is a negative value.

After the convolutional layers, a pooling layer was added to minimize the information and simplify the classification process. The method used was the average pooling, which calculates the mean value of a predetermined set of points and creates a new sequence only with the mean values, decreasing the amount of information [Fawaz 2020].

The next layers are classifying layers that are composed by a simpler model called multilayer perceptron (MLP). The basic unit of this model is the perceptron neuron that receives an input and calculates the output with a function based on the set of parameters given by the previous layers and it passes to an activation function (to give a non linear characteristic to the model) and to the following neurons in the next layer. All neurons in each layer are connected to all neurons in the next layer, the last having the number of neurons equal to the number of classifications to output the prediction of the model. Dropout layers can be placed between any layer and deactivate a preset number of neurons in the layer, forcing the model to create new paths to solve the problem and predict values, increasing its robustness [Taud and Mas 2017]. Figure 2 shows the architecture proposed in this work.

The cited process is repeated a set amount of times (200 epochs), and after each epoch, the model tests its performance in the validation set (simulating a real situation with unknown samples) to adjust the values of the previous layers in a process called backpropagation, to improve its metrics until it reaches the peak of its capacity, converging the prediction error to a minimum.

2.4. Model evaluation

To evaluate the model performance, a checkpoint function is used that saves the best model found in the training using a predetermined metric, in this case being the model with the minimum validation set loss of information, avoiding overfitting in the saved models and finding the best accuracy possible with the information available. The saved models were evaluated using the loss and accuracy curves along the epochs and the confusion matrix of the validation set.

With these curves, it is possible to analyze the learning capacity of the model, with the maximum accuracy and the minimum loss of information reached. Also, it is possible to identify overfitting, when the accuracy curves of the training set continue to raise while the validation set starts to decrease due to the model memorizing the classifications of the training samples and not having the capacity to generalize the patterns learned. The noise in the curves also shows the consistency in the learning process, high noise meaning a higher difficulty to learn new patterns consistently.

The confusion matrix is a matrix with the lines representing the real predictions and the columns representing the model predictions for a number of samples. The values that are positioned in the main diagonal of the matrix are the correct predictions, all of the other values are erroneous predictions made by the model. With this matrix it is possible to find the accuracy, precision, recall and F1-score of the model, which helps the analysis of the classification and generalization power of the model.

The best models were tested again with the previously separated test set of the dataset to avoid bias in the evaluation. The best model was evaluated with a confusion matrix based on the four metrics previously cited.

3. Results and Discussion

Here we used the network architecture based on the papers [Wang et al. 2017] and [Fawaz 2020], with an increase in the number of convolutional layers, a change in the number of filters and the addition of an MLP model at the top of the CNN to achieve best metrics.

This architecture uses an Adam optimizer, with an initial learning rate of 0.001 with a reduction factor of 0.5 after 5 epochs without improvement in the validation set loss metric, meaning the learning rate decreases by 50% if the metric does not improve. The model was trained for 200 epochs, and an early stopping function was used to stop the training if the metrics did not improve in 20 epochs. The architecture presented a noisy curve for both the accuracy and the loss metrics, which means that the learning was not as constant as desired, even though the validation curves followed the training curves, representing a good generalization power, as shown in Figure 3.

The model precision was maintained above 80% (especially by the MI and CD classes that presented precision values near 90%), the confusion matrix generated by the validation set (containing 2762 records) also shows difficulties for the classification of some classes, such as hypertrophy (HYP), that did not achieve satisfactory recall metrics (39.5%).

Generally, the model presented a satisfactory accuracy of 82.7% in the validation set, being the best accuracy achieved during the different configuration tests. The saved

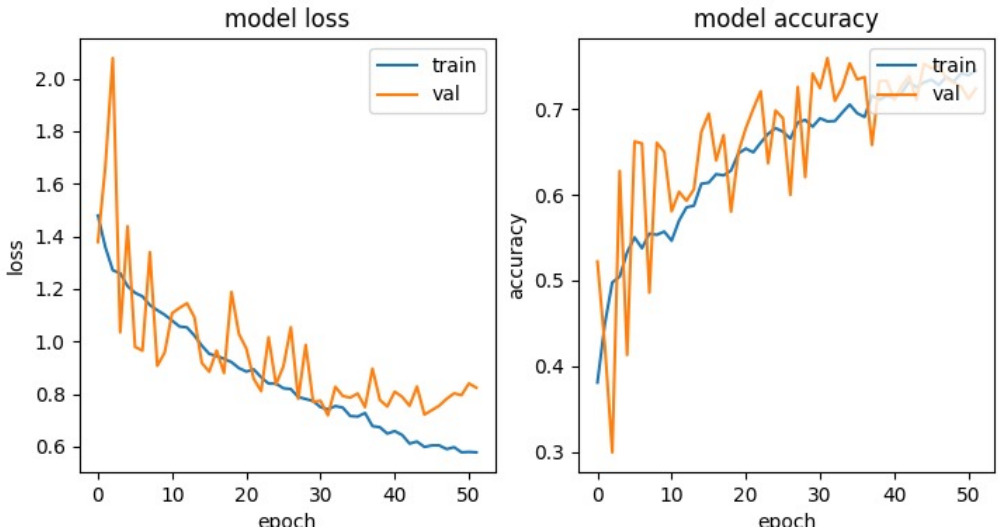

Figure 3. Model accuracy and loss curves.

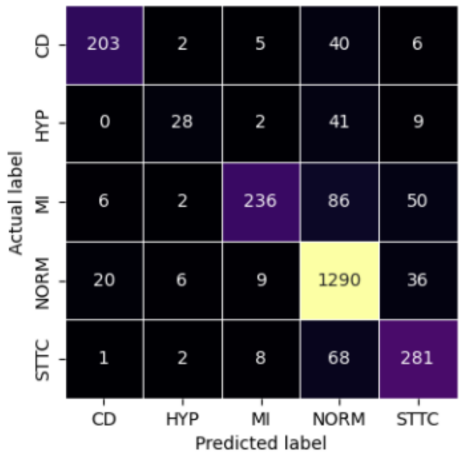

Figure 4. Confusion matrix of the test set.

model was loaded and tested with the test set, containing 2437 unknown records for the model, and achieved a precision of 81.39 %, 69.71 % recall, 73.38 % F1-score and 83.6% accuracy, presented by the confusion matrix of the test set shown in figure 4 and Table 1.

The model presented a great precision in normal (NORM), myocardial infarction (MI) and conduction disturbance (CD) records and a poorer precision in the hypertrophy (HYP) class, achieving 70 % precision. The best recall found was for normal records, achieving a metric of 94.7 % while other classes presented values between 60 % and 80 %, with the exception of the hypertrophy class that presented a low value of 35 %.

The F1-score metric presented a similar value to the recall metric, with the normal class obtaining the highest value (89.3 %) and the hypertrophy class presenting a lower value (44.66 %). All other classes maintained average results of 73 % to 84 %.

Summarizing these results, it is possible to identify a great capacity to classify non-pathological signals. However, the model has great difficulty identifying hypertrophy and this could be attributed to several factors, most likely the lack of sufficient samples in

Table 1. Confusion matrix metrics.

Condition	Precision	Recall	F1-Score	Accuracy
CD	88.2%	79.29%	83.5%	–
HYP	70%	35%	44.66%	–
MI	90.7%	62.1%	73.72%	–
NORM	84.5%	94.7%	89.3%	–
STTC	73.56%	78.05%	75.73%	–
Mean	81.39%	69.71%	73.38	83.6%

the training set.

Since heart hypertrophy is the minority class in the dataset, with only 80 records with this classification in the test set (compared to 1361 normal records) and its disturbances in the ECG are subtle (with the exception of right ventricle hypertrophy, which presents itself as an inversion of the signal in the III derivation), the model has a great difficulty learning the patterns that are characteristic of this pathology. Even with the balancing function, the class has much fewer samples than the other classes, creating a bias because there are not enough samples to learn patterns from, forcing the model to use the learned parameters from other classes in training and ignoring subtle changes from this category.

The performance of the model can also be compared to related papers, to understand how great is the classification capacity and what their differences are. It is important to note that although the methods are similar, a large part of the studies are based on different datasets, which means that it is not possible to compare them directly. The articles with more similarity are those presented by [Śmigiel et al. 2021] and [Bhanjaa and Khampariya 2023], which have a similar methodology and use the same dataset as in the present study.

[Hasan and Bhattacharjee 2019], besides using 3 different datasets (MIT-BIH, St.-Petersburg arrhythmia database and PTB Diagnostic ECG Database) that have different signal formats, being a 16-lead record, one of them being the respiratory frequency and the other being the input voltage in the equipment, also uses a preprocessed signal, with empiric mode decomposition (EMD) that separates the complex waves in different components to facilitate analysis. The study achieved an accuracy above 98 % in all datasets.

[Śmigiel et al. 2021] paper uses the PTB-XL dataset and a convolutional neural network approach with 3 methodologies. The best methodology found in the study is with a CNN with entropy parameters, that achieved 89.2% accuracy across 2 categories. To directly compare to the present study, the paper also presents metrics for the classification of 5 categories, the model achieving an accuracy of 76.5%, showing that the model of the present study has a greater capability of classifying the raw data of the records.

[Bhanjaa and Khampariya 2023], present 2 approaches with one-dimensional AlexNet and LeNet based algorithms. The records were filtered using a Savitzky-Golay

filter to reduce noise and facilitate signal classification, achieving an accuracy of 97.5% for the AlexNet based algorithm and 94.2% for the LeNet base algorithm, showing that data pre-processing together with a complex network has a great impact on signal classification compared to the present study.

4. Conclusion

The use of artificial intelligence in healthcare is being explored for a short time and has several applications that may benefit from further studies. The proposed neural network has great value in reducing diagnostic time with a satisfactory accuracy of almost 84%, presenting a better classification capacity than similar studies without the use of filters. Despite the previous affirmation, more studies are still needed to increase the network classification capacity (achieving a similar capacity to networks that classify filtered signals), especially for hypertrophy pathologies, and to develop ways to classify individual conditions instead of general classes with similar accuracy.

Acknowledgments

We thank the anonymous reviewers for their valuable feedback. This research was partially funded and supported by Coordenação de Aperfeiçoamento de Pessoal de Nível Superior - Brasil (CAPES) - Finance Code 001, Conselho Nacional de Desenvolvimento Científico e Tecnológico - CNPq (grants 313845/2023-9, and 404572/2021-9), and the Competence Center on Digital Agriculture, with financial resources from PPI HardwareBR of the MCTI grant number 056/2023, signed with EMBRAPII.

References

Ayadi, W., Elhamzi, W., Charfi, I., and Atri, M. (2021). Deep cnn for brain tumor classification. *Neural processing letters*, 53:671–700.

Bhanjaa, M. N. and Khampariya, P. (2023). Design and comparison of deep learning model for ecg classification using ptb-xl dataset.

Bian, Y., Chen, J., Chen, X., Yang, X., Chen, D. Z., and Wu, J. (2023). Identifying electrocardiogram abnormalities using a handcrafted-rule-enhanced neural network. *IEEE/ACM Transactions on Computational Biology and Bioinformatics*, 20(4):2434–2444.

Eren, L., Ince, T., and Kiranyaz, S. (2019). A generic intelligent bearing fault diagnosis system using compact adaptive 1d cnn classifier. *Journal of Signal Processing Systems*, 91(2):179–189.

Fabian, P. (2011). Scikit-learn: Machine learning in python. *Journal of machine learning research 12*, page 2825.

Fawaz, H. I. (2020). Deep learning for time series classification. *arXiv preprint arXiv:2010.00567*.

Hall, J. E. (2021). *Guyton & Hall. Tratado de fisiología médica*. Elsevier Health Sciences.

Hasan, N. I. and Bhattacharjee, A. (2019). Deep learning approach to cardiovascular disease classification employing modified ecg signal from empirical mode decomposition. *Biomedical signal processing and control*, 52:128–140.

Kaplan, J. D., Evans, G., Foster, E., Lim, D., and Schiller, N. B. (1994). Evaluation of electrocardiographic criteria for right atrial enlargement by quantitative two-dimensional echocardiography. *Journal of the American College of Cardiology*, 23(3):747–752.

Khan, A., Sohail, A., Zahoora, U., and Qureshi, A. S. (2020). A survey of the recent architectures of deep convolutional neural networks. *Artificial intelligence review*, 53:5455–5516.

Kusuma, S. and Udayan, J. D. (2020). Analysis on deep learning methods for ecg based cardiovascular disease prediction. *Scalable Computing: Practice and Experience*, 21(1):127–136.

Lu, J., Tan, L., and Jiang, H. (2021). Review on convolutional neural network (cnn) applied to plant leaf disease classification. *Agriculture*, 11(8):707.

Maccagnan, G. C., Schmith, J., Santos, M., and de Figueiredo, R. M. (2023). Toolbox for vessel x-ray angiography images simulation. In *Anais do XXIII Simpósio Brasileiro de Computação Aplicada à Saúde*, pages 59–70. SBC.

Maione, C. et al. (2020). Balanceamento de dados com base em oversampling em dados transformados.

Nyholm, B. C., Ghouse, J., Lee, C. J.-Y., Rasmussen, P. V., Pietersen, A., Hansen, S. M., Torp-Pedersen, C., Køber, L., Haunsø, S., Olesen, M. S., et al. (2022). Fascicular heart blocks and risk of adverse cardiovascular outcomes: Results from a large primary care population. *Heart Rhythm*, 19(2):252–259.

Pastore, A. C., Samesima, N., Tobias, N. M. M. d. O., and Pereira Filho, H. G. (2016). Eletrocardiografia atual: curso do serviço de eletrocardiografia do incor. In *Eletrocardiografia atual: curso do serviço de eletrocardiografia do InCor*, pages 413–413.

Prati, R. C., Batista, G., Monard, M. C., do Trabalhador Sao-Carlense, A., and Postal, C.-C. (2003). Uma experiência no balanceamento artificial de conjuntos de dados para aprendizado com classes desbalanceadas utilizando análise roc. In *Proc. of the Workshop on Advances & Trends in AI for Problem Solving*, volume 1, pages 28–33.

Rose, L. and Kuhn, L. (2009). Ecg interpretation part 2: determination of bundle branch and fascicular blocks. *Journal of Emergency Nursing*, 35(2):123–126.

Śmigiel, S., Pałczyński, K., and Ledziński, D. (2021). Ecg signal classification using deep learning techniques based on the ptb-xl dataset. *Entropy*, 23(9):1121.

Taud, H. and Mas, J.-F. (2017). Multilayer perceptron (mlp). In *Geomatic approaches for modeling land change scenarios*, pages 451–455. Springer.

Thygesen, K., Alpert, J. S., Jaffe, A. S., Simoons, M. L., Chaitman, B. R., and White, H. D. (2012). Third universal definition of myocardial infarction. *Circulation*, 126(16):2020–2035.

Tortora, G. J. and Derrickson, B. H. (2018). *Principles of anatomy and physiology*. John wiley & sons.

Tsao, C. W., Josephson, M. E., Hauser, T. H., O'Halloran, T. D., Agarwal, A., Manning, W. J., and Yeon, S. B. (2008). Accuracy of electrocardiographic criteria for atrial

enlargement: validation with cardiovascular magnetic resonance. *Journal of Cardiovascular Magnetic Resonance*, 10(1):7.

Wagner, P., Strodthoff, N., Bousseljot, R.-D., Kreiseler, D., Lunze, F. I., Samek, W., and Schaeffter, T. (2020). Ptb-xl, a large publicly available electrocardiography dataset. *Scientific data*, 7(1):1–15.

Wang, Z., Yan, W., and Oates, T. (2017). Time series classification from scratch with deep neural networks: A strong baseline. In *2017 International joint conference on neural networks (IJCNN)*, pages 1578–1585. IEEE.

Wilmore, J. H., Costill, D. L., and Kenney, W. L. (2004). *Physiology of sport and exercise*, volume 20. Human kinetics Champaign, IL.

Xie, C., McCullum, L., Johnson, A., Pollard, T., Gow, B., and Moody, B. (2022). Waveform database software package (wfdb) for python. *PhysioNet*.